On turbulent mixing in stably stratified wall-bounded flows

Farid Karimpour and Subhas Karan Venayagamoorthy

Citation: Physics of Fluids (1994-present) **27**, 046603 (2015); doi: 10.1063/1.4918533
View online: http://dx.doi.org/10.1063/1.4918533
View Table of Contents: http://scitation.aip.org/content/aip/journal/pof2/27/4?ver=pdfcov
Published by the AIP Publishing

PHYSICS OF FLUIDS **27**, 046603 (2015)

On turbulent mixing in stably stratified wall-bounded flows

Farid Karimpour and Subhas Karan Venayagamoorthy[a)]
Department of Civil and Environmental Engineering, Colorado State University, Fort Collins, Colorado 80523-1372, USA

(Received 20 October 2014; accepted 3 April 2015; published online 17 April 2015)

In this paper, we provide an analysis of turbulent mixing in stably stratified wall-bounded flows to highlight a number of important issues such as prediction of the turbulent viscosity, the turbulent diffusivity, and the irreversible flux Richardson number. By invoking the equilibrium assumption between the production rate of the turbulent kinetic energy (P), the dissipation rate of the turbulent kinetic energy (ϵ), and the turbulent potential energy dissipation rate (ϵ_{PE}) as $P \approx \epsilon + \epsilon_{PE}$ and also assuming equilibrium between the buoyancy flux (B) and ϵ_{PE} as $-B \approx \epsilon_{PE}$, we first propose that the irreversible flux Richardson number ($R_f^* = \epsilon_{PE}/(\epsilon + \epsilon_{PE})$) can be approximated with the flux Richardson number ($R_f = -B/P$), especially for low gradient Richardson numbers. Second, we propose that the turbulent viscosity $\nu_t \approx (1 - R_f^*)^{-1}\epsilon/S^2$, where S is the mean shear rate. We then extend our analysis to propose appropriate velocity and length scales. Tests using the direct numerical simulation (DNS) data of turbulent channel flow of García-Villalba and del Álamo ["Turbulence modification by stable stratification in channel flow," Phys. Fluids **23**, 045104 (2011)] are performed to evaluate our propositions. The comparisons between the exact turbulent viscosity, length and velocity scales, and the proposed formulations are excellent. Also, the agreement between R_f and R_f^* is reasonable for the bulk of the flow depth with differences of about 20% on average, except at depths very close to the flow boundaries. Finally, by invoking the equilibrium assumption between the buoyancy flux (B) and the dissipation rate of the turbulent potential energy (ϵ_{PE}) as $-B \approx \epsilon_{PE}$, we infer the turbulent diffusivity as $\kappa_t \approx \epsilon_{PE}/N^2$, where N is the buoyancy frequency. The comparison of the proposed turbulent diffusivity with the exact turbulent diffusivity computed from DNS data is good especially close to the wall but the agreement deteriorates far away from the wall, indicating the breakdown of assuming equilibrium as $-B \approx \epsilon_{PE}$ which is attributed to the presence of linear internal wave motions in this far-wall region. © *2015 AIP Publishing LLC.* [http://dx.doi.org/10.1063/1.4918533]

I. INTRODUCTION

Most geophysical flows such as those in estuaries or the atmosphere to the more complicated flows in lakes and oceans are influenced by both the density stratification and the bottom boundary. In such flows, the simultaneous existence of the density stratification and the solid wall results in anomalous mixing of momentum and active scalar (density) compared to other turbulent flows. Hence, it is not surprising that stratified wall-bounded flows are usually considered as one of the most complex turbulent flows and have been the subject of several studies. For example, Arya[1] ran experiments to study well-developed stratified flat boundary layer flow and observed that mean velocity and temperature profiles were influenced by thermal stratification in the inner and outer layers. Komori *et al.*[2] experimentally investigated the effect of stable stratification on turbulence in an open channel flow. Their observations showed wavelike motions of turbulent quantities in regions away from the wall. Garg *et al.*[3] and Armenio and Sarkar[4] performed large-eddy simulations (LES) to study stably stratified pressure-gradient-driven channel flows. Nieuwstadt[5] used

a)Email: vskaran@colostate.edu

direct numerical simulation (DNS) to study atmospheric boundary layer flows under very strong stratification where turbulence can hardly survive. Taylor *et al.*[6] performed LES of stably stratified open channel flow to investigate different aspects of turbulence such as the behavior of the buoyancy flux, mixing efficiency, and the turbulent Prandtl number. García-Villalba and del Álamo[7] performed DNS of stably stratified wall-bounded flows for a varying range of density stratification to investigate turbulence modification. Their study showed that velocity profiles change with the increasing stratification and deviate from the (classical) neutral case. They also noted that under weakly stratified conditions, the near-wall region stayed unaffected while turbulence was modified in the core of the channel. On the other hand, for stronger stratifications, turbulent fluxes vanished in the core of the channel and laminar patches appeared in the near-wall region.

Quantifying the mixing of the momentum as well as the diapycnal mixing of density is imperative as they directly impact the state of geophysical flows in both the ocean and the atmosphere. For example, in coupled ocean-atmosphere problems, quantifying the momentum and heat fluxes across the interface is crucial for properly assessing the energetics and associated mixing in the upper ocean. Other examples include mixing and transport of nutrients and other scalars in the ocean. Such processes are sustained by turbulent fluxes. The turbulent (eddy) viscosity (ν_t) and the turbulent (eddy) diffusivity (κ_t) are the two parameters which are widely used for the assessment of the state of the flow (such as turbulent mixing) in physical oceanography or atmospheric sciences and are also employed to quantify the turbulent fluxes in numerical models for simulating stratified turbulent flows. For a uni-directional shear flow, using the turbulent-viscosity hypothesis (TVH), the turbulent viscosity (ν_t) is defined as

$$\nu_t = \frac{-\overline{u'v'}}{\partial \overline{U}/\partial y}, \tag{1}$$

and using the gradient-diffusion hypothesis (GDH), the turbulent diffusivity (κ_t) is given by

$$\kappa_t = \frac{-\overline{\rho'v'}}{\partial \overline{\rho}/\partial y}, \tag{2}$$

where $\overline{U}$ is the mean streamwise velocity, y is the normal distance from the wall, and $\overline{\rho}$ is the fluid mean density.

The turbulent viscosity and diffusivity have to be specified (computed) using turbulence closure schemes. As a result, several parameterizations have been proposed that make use of mean and/or other turbulent quantities. A common approach for parameterization of ν_t and κ_t is to assume stationarity (i.e., statistics are invariant due to change in time) and homogeneity (i.e., statistics are invariant under translations) in the flow. For example, the formulation of ν_t in the k-ϵ model is developed by assuming the balance between the production rate of the turbulent kinetic energy (P), the dissipation rate of the turbulent kinetic energy (ϵ), and the buoyancy flux (B) which is given by[8]

$$\nu_t = \left(1 - R_f\right) C_\mu \frac{k^2}{\epsilon}. \tag{3}$$

Here, $k = \frac{1}{2}(\overline{u'^2} + \overline{v'^2} + \overline{w'^2})$ is the turbulent kinetic energy, ϵ is the dissipation rate of the turbulent kinetic energy, and $C_\mu = (-\overline{u'v'}/k)^2$ is the turbulent viscosity parameter usually taken as $C_\mu \approx 0.09$.[9] R_f is the flux Richardson number that for a shear flow is usually defined as[10]

$$R_f = \frac{-B}{P}, \tag{4}$$

where $B = -g/\rho_0(\overline{\rho'v'})$ is the buoyancy flux and $P = -\overline{u'v'}(\partial \overline{U}/\partial y)$ is the rate of production of k. Osborn and Cox[11] derived an expression for the turbulent diffusivity of temperature by assuming balance between the production and dissipation rates in the evolution equation of the temperature variance. Winters and D'Asaro[12] showed that this assumption can be generalized to any other scalar being diffused in order to derive the relevant turbulent diffusivity. Hence, applying the Osborn and Cox[11] formulation to the scalar (density) variance evolution equation (or alternatively to the

turbulent potential energy evolution equation), it follows that κ_t is given by[13]

$$\kappa_t = \frac{\epsilon_{PE}}{N^2}, \tag{5}$$

where ϵ_{PE} is the dissipation rate of the turbulent potential energy which is defined as

$$\epsilon_{PE} = N^2\left(\frac{\partial\overline{\rho}}{\partial y}\right)^{-2}\epsilon_\rho. \tag{6}$$

It should be noted that the dissipation rate of the turbulent potential energy (ϵ_{PE}) is a direct measure of the irreversible rate of increase of the background potential energy. Here, the background potential energy is the (minimum) potential energy that a stratified flow can have and is not available for conversion to kinetic energy to drive fluid motions.[10] In Eq. (6), $\epsilon_\rho = \kappa\overline{\nabla\rho'.\nabla\rho'}$ is the density (scalar) variance dissipation rate with κ defined as the molecular diffusivity. Also, $N = \sqrt{(-g/\rho_0)(\partial\overline{\rho}/\partial y)}$ is the Brunt-Väisälä or buoyancy frequency which represents the oscillation frequency of a displaced fluid particle about its equilibrium position in a stratified flow.[14] In this equation, g is the gravitational acceleration, ρ_0 is the reference density, and $\partial\overline{\rho}/\partial y$ is the vertical gradient of the mean density.

Besides ν_t and κ_t, the efficiency of mixing is another key parameter in geophysical flows, since it provides a measure of the irreversible diapycnal mixing of density. The irreversible flux Richardson number (R_f^*) was created by Peltier and Caulfield[10] to characterize the efficiency of (irreversible) mixing in stably stratified turbulent flows. To do this, R_f^* is defined based on the irreversible transfer of the turbulent kinetic energy (k) into the background potential energy as follows[15]:

$$R_f^* = \frac{\epsilon_{PE}}{\epsilon + \epsilon_{PE}}. \tag{7}$$

Both ϵ and ϵ_{PE} are positive-definite quantities, ensuring that R_f^* will be limited to $0 \le R_f^* \le 1$. In a stratified flow, the turbulent kinetic energy (k) can be irreversibly lost via two processes, namely: (i) k can be directly lost by internal friction at a rate given by ϵ and (ii) some fraction of k gets converted irreversibly into the background potential energy at a rate given by ϵ_{PE}. For the second process to happen, the turbulent kinetic energy has to be transferred as the buoyancy flux (B). It should be noted that not all of the turbulent kinetic energy (k) transferred via the buoyancy flux (B) in a stratified fluid goes into the background potential energy. A portion of the turbulent kinetic energy (k) goes into increasing the available potential energy which is the amount of potential energy in a stratified flow that is available for conversion to kinetic energy.[10] Hence, defining the irreversible flux Richardson number as R_f^* using Eq. (7) provides a robust formulation for quantifying the irreversible mixing in stably stratified flows that is free from reversible fluxes caused by internal wave motions.

However, even though R_f^* provides a direct measure of the irreversible mixing in a stratified turbulent flow, it is difficult to measure directly. This is due to challenges associated with separating reversible and irreversible changes in the density field from point measurements in a fluid volume. In practice, the flux Richardson number (R_f) is often measured instead of R_f^* and the common assumption that $R_f^* \approx R_f$ is used. However, the common definition of $R_f = -B/P$ incorporates the stirring effects as both B and P inherently consist of reversible fluxes. Therefore, it could be negative for non-stationary strongly stably stratified flows where countergradient fluxes are noticeable.[15] Hence, this common substitution is still a matter of doubt and needs more investigation in order to ascertain the conditions under which these two quantities may be used interchangeably.

In this paper, we evaluate the suitability of invoking the equilibrium assumptions for inference of R_f^*, ν_t, and κ_t in stably stratified wall-bounded flows. In Sec. II, we present the evolution equations of the turbulent kinetic energy and scalar (density) variance. We derive a revised formulation for the turbulent viscosity (ν_t) for a stably stratified turbulent channel flow by using the equilibrium assumption (i.e., $P \approx \epsilon + \epsilon_{PE}$) all the way to the wall. Dimensional arguments are then used to propose appropriate (relevant) velocity and length scales. In Sec. III, the validity of the propositions is evaluated by performing tests using turbulent channel flow DNS data. First, the behavior of R_f is compared with R_f^*. Second, the validity of the proposed ν_t and relevant scales are evaluated. In

Sec. IV, the equilibrium between the buoyancy flux and the dissipation rate of the turbulent potential energy is invoked (i.e., $-B \approx \epsilon_{PE}$) which leads to Osborn and Cox[11] formulation for κ_t. The suitability of this formulation for estimating κ_t in stably stratified wall-bounded flows is evaluated by performing tests using DNS data. Conclusions are given in Sec. V.

II. PREDICTION OF THE TURBULENT VISCOSITY

A. Evolution equations

The evolution equations for the turbulent kinetic energy (k) and the density (scalar) variance ($\overline{\rho'^2}$) for an inhomogeneous stratified shear flow with the Boussinesq approximation can be, respectively, written as

$$\frac{\partial k}{\partial t} + \overline{U_j}\frac{\partial k}{\partial x_j} = P - \epsilon + B + D_\nu + T + \Pi, \tag{8}$$

$$\frac{\partial \left(\frac{1}{2}\overline{\rho'^2}\right)}{\partial t} + \overline{U_j}\frac{\partial \left(\frac{1}{2}\overline{\rho'^2}\right)}{\partial x_j} = P_\rho - \epsilon_\rho + T_\rho, \tag{9}$$

where $P = (-\overline{u_i'u_j'})\partial\overline{U_i}/\partial x_j$ is the production rate of k, $\epsilon = \nu(\overline{\partial u_i'/\partial x_j)(\partial u_i'/\partial x_j)}$ $+ \nu(\overline{\partial u_i'/\partial x_j)(\partial u_j'/\partial x_i)}$ is the dissipation rate of k, $B = (-g/\rho_0)(\overline{\rho' v'})$ is the buoyancy flux, $D_\nu = \nu(\partial^2 k/\partial x_j^2)$ is the viscous diffusion of k, $T = -(1/2)\partial(\overline{u_j'u_i'u_i'})/\partial x_j$ is the divergence of the turbulent convection of k, and $\Pi = -(1/\rho_0)\partial(\overline{p'u_j'})/\partial x_j$ is the divergence of the pressure flux, respectively. $P_\rho = (-\overline{\rho'u_j'})\partial\overline{\rho}/\partial x_j$ is the production rate of the density variance, $\epsilon_\rho = \kappa(\overline{\partial\rho'/\partial x_j)(\partial\rho'/\partial x_j)}$ is the dissipation rate of the density variance, and $T_\rho = -(1/2)\partial(\overline{\rho'^2u_j'})/\partial x_j$ is the divergence of the density variance flux. The divergences of fluxes D_ν, T, and Π are also known as the viscous transport of k, the turbulent velocity transport (turbulent convection) of k, and the pressure transport of k, respectively.[16] The divergences of fluxes (or transport terms) in the turbulent kinetic energy and density variance equations arise due to the inhomogeneity in the flow.

Also, by multiplying the evolution equation of the density variance introduced in Eq. (9) into $N^2(\partial\overline{\rho}/\partial y)^{-2}$, the evolution equation of the turbulent potential energy (E'_{PE}) can be derived as

$$\frac{\partial E'_{PE}}{\partial t} + \overline{U_j}\frac{\partial E'_{PE}}{\partial x_j} = -B - \epsilon_{PE} + T_{PE}, \tag{10}$$

where the turbulent potential energy is

$$E'_{PE} = N^2\left(\frac{\partial\overline{\rho}}{\partial y}\right)^{-2}\left(\frac{1}{2}\overline{\rho'^2}\right). \tag{11}$$

Note in Eq. (10), ϵ_{PE} is the dissipation rate of the turbulent potential energy and T_{PE} $= N^2(\partial\overline{\rho}/\partial y)^{-2}T_\rho$ is the divergence of the turbulent potential energy flux (or transport rate of the turbulent potential energy).

The evolution equation of the total turbulent energy (E'_T) can be obtained by adding the evolution equations for the turbulent kinetic energy (Eq. (8)) and the turbulent potential energy (Eq. (10)) as

$$\frac{\partial E'_T}{\partial t} + \overline{U_j}\frac{\partial E'_T}{\partial x_j} = P - \epsilon - \epsilon_{PE} + D_\nu + T + \Pi + T_{PE}. \tag{12}$$

As it can be seen, the buoyancy flux (B) is absent in this equation. In Eq. (10), $\epsilon_T = \epsilon + \epsilon_{PE}$ is the dissipation rate of the total turbulent energy and $T_T = D_\nu + T + \Pi + T_{PE}$ is the total of the transport terms of the total turbulent energy.

B. Equilibrium assumption

For steady, fully developed stratified wall-bounded turbulent flows, Eqs. (8) and (10) simplify to

$$P = -\overline{u'v'}\frac{d\overline{U}}{dy} = \epsilon - B - D_\nu - T - \Pi, \tag{13}$$

$$-B = \frac{-g}{\rho_0}\left(\overline{\rho' v'}\right) = \epsilon_{PE} - T_{PE}. \tag{14}$$

Equation (13) implies that the production rate of k is balanced by the buoyancy flux, the dissipation rate of k, and the divergences of fluxes. Similarly, Eq. (14) means that the production rate of E'_{PE} (which is $-B$) is balanced by the dissipation rate of the turbulent potential energy and also its flux divergence, when the flow is stationary. Using the TVH, Eq. (13) can be rewritten as

$$\nu_t = \frac{\epsilon - B - D_\nu - T - \Pi}{S^2}, \tag{15}$$

which (by using $B = -PR_f$) can be recast as

$$\nu_t = \left(\frac{1}{1 - R_f}\right)\frac{\epsilon - D_\nu - T - \Pi}{S^2}. \tag{16}$$

Similarly, using the GDH, Eq. (14) can be recast in terms of the turbulent diffusivity (κ_t) as follows

$$-B = \kappa_t N^2 = \epsilon_{PE} - T_{PE}. \tag{17}$$

We can now express the flux Richardson number (R_f) as

$$R_f = \frac{-B}{P} = \frac{\epsilon_{PE} - T_{PE}}{\epsilon + \epsilon_{PE} - D_\nu - T - \Pi - T_{PE}}. \tag{18}$$

By substituting the buoyancy flux (B) given by Eq. (17) into Eq. (15), ν_t can be rewritten as

$$\nu_t = \frac{(\epsilon + \epsilon_{PE}) - (D_\nu + T + \Pi + T_{PE})}{S^2}, \tag{19}$$

which can be further simplified to yield

$$\begin{aligned}\nu_t &= \left(\frac{1}{1 - \frac{\epsilon_{PE}}{\epsilon + \epsilon_{PE}}}\right)\frac{\epsilon}{S^2} - \frac{D_\nu + T + \Pi + T_{PE}}{S^2} \\ &= \left(\frac{1}{1 - R_f^*}\right)\frac{\epsilon}{S^2} - \frac{D_\nu + T + \Pi + T_{PE}}{S^2}.\end{aligned} \tag{20}$$

Here, R_f^* is the irreversible flux Richardson number given by Eq. (7).

Let us for now assume that the total of all the transport terms (i.e., $T_T = D_\nu + T + \Pi + T_{PE}$) is negligible in comparison with the dissipation rate of the total turbulent energy (i.e., $\epsilon_T = \epsilon + \epsilon_{PE}$). This implies that $\epsilon + \epsilon_{PE} \gg D_\nu + T + \Pi + T_{PE}$ and hence the evolution equation for the turbulent kinetic energy (or alternatively the total turbulent energy evolution equation) simplifies to $P \approx \epsilon + \epsilon_{PE}$. Townsend[17] described the equality between the production and dissipation terms as the "equilibrium assumption" which occurs in equilibrium layers of wall-bounded flows. The validity of this assumption will be tested in Sec. III B. Now, by using the equilibrium assumption in the denominator of Eq. (18) (i.e., assuming $P \approx \epsilon + \epsilon_{PE}$), R_f can be approximated as shown in

$$R_f = \frac{-B}{P} \approx \frac{\epsilon_{PE}}{\epsilon + \epsilon_{PE}} - \frac{T_{PE}}{\epsilon + \epsilon_{PE}}. \tag{21}$$

Now, if we also use the equilibrium assumption in the numerator as $-B \approx \epsilon_{PE}$ which implies that $T_{PE} \ll \epsilon_{PE}$, then it follows that R_f is approximately equal to R_f^* as shown in

$$R_f = \frac{-B}{P} \approx R_f^* = \frac{\epsilon_{PE}}{\epsilon + \epsilon_{PE}}. \tag{22}$$

We will show later in Sec. IV B that this assumption (i.e., $-B \approx \epsilon_{PE}$ or $T_{PE} \ll \epsilon_{PE}$) does not strictly hold across the flow depth. Also, by using the equilibrium assumption as $P \approx \epsilon + \epsilon_{PE}$, ν_t given in Eqs. (19) and (20) simplifies to

$$\nu_t \approx \frac{\epsilon + \epsilon_{PE}}{S^2} = \left(\frac{1}{1 - R_f^*}\right)\frac{\epsilon}{S^2}. \tag{23}$$

The implication of the equilibrium assumption implied by $P \approx \epsilon + \epsilon_{PE}$ is that $\nu_t \approx (\epsilon + \epsilon_{PE})/S^2$. Also, imposing the additional equilibrium assumption given by $-B \approx \epsilon_{PE}$ implies that the flux Richardson number (R_f) and the irreversible flux Richardson number (R_f^*) should be approximately equal (i.e., $R_f \approx R_f^*$). We test the validity of these propositions in Sec. III.

C. Relevant velocity and length scales

Here, we discuss the relevant velocity and length scales in the context of the TVH that define the turbulent viscosity (ν_t) in stably stratified wall-bounded turbulent flows. Using dimensional analysis, the turbulent viscosity (ν_t) can be recast in terms of velocity, length, and time scales as

$$\nu_t = U_{TVH}.L_{TVH} = U_{TVH}^2.T_{TVH} = L_{TVH}^2/T_{TVH}, \tag{24}$$

where U_{TVH} is the characteristic velocity scale proposed by Pope[16] as $|\overline{u'v'}|^{1/2}$, L_{TVH} is the characteristic length scale, and T_{TVH} is the characteristic time scale. From the TVH, it is clear that

$$-\overline{u'v'} = U_{TVH}^2 = \nu_t S. \tag{25}$$

Now, by invoking the equilibrium assumption (i.e., $P \approx \epsilon + \epsilon_{PE}$) and therefore using $\nu_t \approx 1/(1 - R_f^*)\epsilon/S^2$, Eq. (25) can be rewritten as

$$U_{TVH}^2 \approx U_S^2 = \left(\frac{1}{1 - R_f^*}\right)\left(\frac{\epsilon}{S^2}\right)S, \tag{26}$$

where U_S is an approximation for U_{TVH}. Hence, the velocity scale (U_S) can be defined as

$$U_{TVH} \approx U_S = \left(\frac{\epsilon + \epsilon_{PE}}{S}\right)^{1/2} = \left(\frac{1}{1 - R_f^*}\right)^{1/2}\left(\frac{\epsilon}{S}\right)^{1/2}. \tag{27}$$

Now, using Eqs. (23), (24), and (27), the length scale (L_{TVH}) can be approximated as

$$\begin{aligned} L_{TVH} &= \frac{\nu_t}{U_{TVH}} = \frac{\left(-\overline{u'v'}\right)^{1/2}}{S} \\ &\approx L_S = \frac{\nu_t}{U_s} = \frac{(\epsilon + \epsilon_{PE})/S^2}{((\epsilon + \epsilon_{PE})/S)^{1/2}} \\ &= \left(\frac{\epsilon + \epsilon_{PE}}{S^3}\right)^{1/2} = \left(\frac{1}{1 - R_f^*}\right)^{1/2}\left(\frac{\epsilon}{S^3}\right)^{1/2}, \end{aligned} \tag{28}$$

where L_S is an approximation for L_{TVH}. It should be noted that for an unstratified flow (i.e., $R_f = 0$), $L_S = (\epsilon/S^3)^{1/2}$ is the classical Corrsin length scale, L_c.[18] The Corrsin length scale is usually taken to denote the upper limit of the inertial subrange (when described in terms of length scales) and is considered to be the smallest eddy size that can be deformed by the mean shear rate.[19] Thus, in unstratified flows, L_c may be interpreted as an equilibrium length scale where $P \approx \epsilon$. Extending this argument to the present context, L_S can be considered as a modified Corrsin length scale for stably stratified flows, which implies that it is the pertinent length scale of the flow when equilibrium holds (i.e., $P \approx \epsilon + \epsilon_{PE}$).

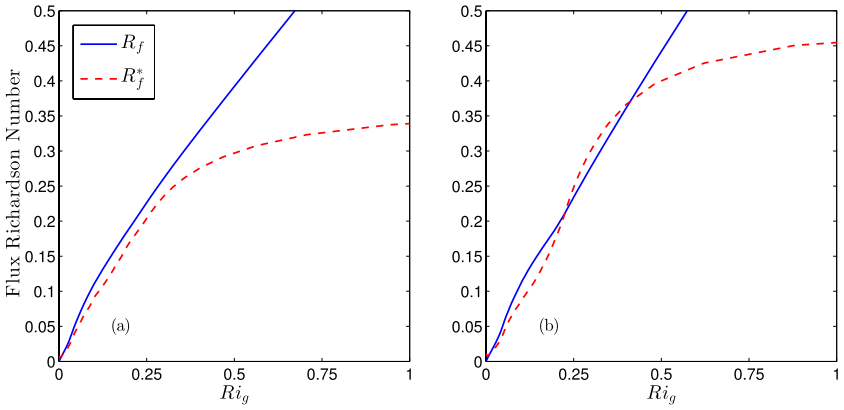

FIG. 1. Comparison of the flux Richardson number (R_f) and the irreversible flux Richardson number (R_f^*) versus Ri_g in a turbulent channel flow at $Re_\tau = 550$ and (a) $Ri_\tau = 60$ and (b) $Ri_\tau = 120$, computed from the DNS data of García-Villalba and del Álamo.[7]

III. TESTS USING DNS DATA

In this section, we first compare the behavior of R_f with R_f^* in order to evaluate the conditions and extent of the flow regime where $R_f \approx R_f^*$ holds. We also assess the validity of the proposed formulation for ν_t shown in Eq. (23). This is followed by an assessment of the validity of the proposed velocity and length scales. The tests are done using the stably stratified turbulent channel flow DNS dataset of García-Villalba and del Álamo[7] with a friction Reynolds number of $Re_\tau = u_\tau \delta/\nu = 550$ for different initial stratifications given by friction Richardson numbers of $Ri_\tau = |\Delta\rho| g\delta/\rho_0 u_\tau^2 = 0,\ 60,$ and 120. Here, u_τ is the friction velocity, δ is half of the channel depth, ν is the kinematic (molecular) viscosity, and $|\Delta\rho|$ is the initial density difference between the bottom of the channel ($y = 0$) and the free-stream ($y = \delta$).

A. Prediction of the irreversible flux Richardson number

In Sec. II B, we have analytically shown that in a stratified channel flow, the irreversible flux Richardson number ($R_f^* = \epsilon_{PE}/(\epsilon + \epsilon_{PE})$) could be approximated with the flux Richardson number given by $R_f = -B/P$, provided that the equilibrium assumptions hold (i.e., $P \approx \epsilon + \epsilon_{PE}$ and $-B \approx \epsilon_{PE}$). The comparison between R_f and R_f^* is shown as a function of the gradient Richardson number ($Ri_g = N^2/S^2$) in Figure 1. A plot of Ri_g versus nondimensional flow depth (y/δ, not shown here) indicates that $Ri_g \leq 1$ for $y/\delta \lesssim 0.95$. As it can be seen from Figure 1, for $Ri_g \lesssim 0.25$, both quantities closely follow each other and grow almost linearly with Ri_g. It is also evident that when $Ri_g > 0.25$, R_f and R_f^* deviate from each other and is an indication that the reversible fluxes are no longer negligible.

Interestingly, the departure between R_f and R_f^* occurs around $Ri_g \approx 0.25$ which is also the commonly assumed value for the critical Richardson number (Ri_{gc}). For stably stratified flows, it is common to consider $Ri_g = 0.25$ as a critical Richardson number for the onset of instabilities. The critical gradient Richardson number of $Ri_{gc} = 0.25$ was derived for the first time by Miles[20] and Howard[21] and denotes the threshold of linear stability for a stably, stratified, two-dimensional flow. While there is still no consensus on the exact value of Ri_{gc} for high Reynolds number stably stratified flows, values in the range of 0.1-1 have been proposed.[22] It is commonly hypothesized that for $Ri_g < Ri_{gc}$, the mean shear rate dominates the restoring buoyancy forces due to density stratification, triggering the onset of Kelvin-Helmholtz instabilities and consequently generation of turbulence. In regions of low Ri_g, irreversible turbulent mixing results in an increase of the background potential energy. For $Ri_g > Ri_{gc}$, linear internal waves and countergradient fluxes persist causing reversible exchanges between the turbulent kinetic energy (k) and the available potential energy. The effect of linear internal waves on scalar mixing will be discussed in Sec. IV B. It seems plausible from these

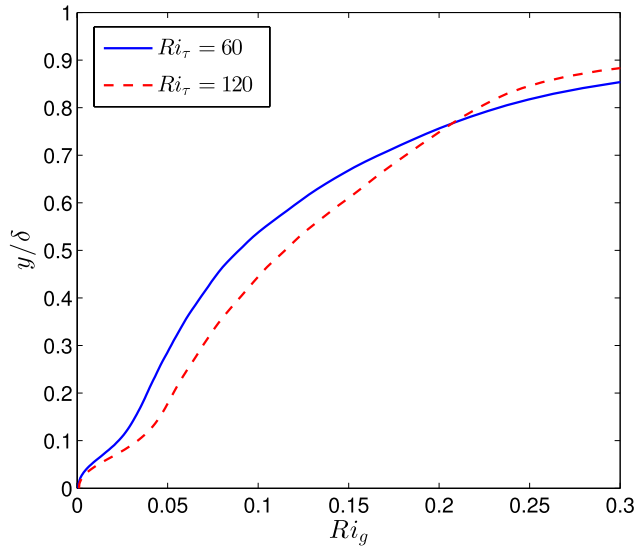

FIG. 2. Ri_g as a function of depth for a turbulent channel flow at $Re_\tau = 550$ and $Ri_\tau = 60, 120$, computed from the DNS data of García-Villalba and del Álamo.[7] Here, δ is half of the channel depth.

results to suggest that the reversible fluxes can be neglected when the gradient Richardson number is below Ri_{gc} with the turbulence generated through shear instabilities, and hence $R_f \approx R_f^*$.

It is clear from Figure 1 that $R_f \approx R_f^*$ for $Ri_g \lesssim 0.25$. However, an important follow-up question is to determine for what fraction of the flow depth does this approximation hold? To answer this question, Ri_g is plotted as a function of the flow depth in Figure 2. It is clear from Figure 2 that for the bulk of the flow depth (almost 85%), the gradient Richardson number (Ri_g) falls below the critical value of 0.25. Figure 3 shows the comparison of R_f and R_f^* as a function of depth. It can be seen that there is reasonable agreement between R_f and R_f^* for almost 90% of the flow depth. Figure 4 shows the normalized difference between R_f and R_f^* over the flow depth. It can be seen that the differences are on average about 20% over the bulk of the flow depth (i.e., $0.05 \lesssim y/\delta \lesssim 0.9$). It is evident that the agreement deteriorates very close to the wall where the transport terms are no longer negligible. The differences are also large close to the free-stream due to the relaxation of the mean shear rate. These figures imply that the flux Richardson number (R_f) reasonably mimics the behavior of R_f^* in stably stratified turbulent channel flows, except very close to the flow boundaries. It is well known that in the region very close to the wall (commonly known as the near-wall region),

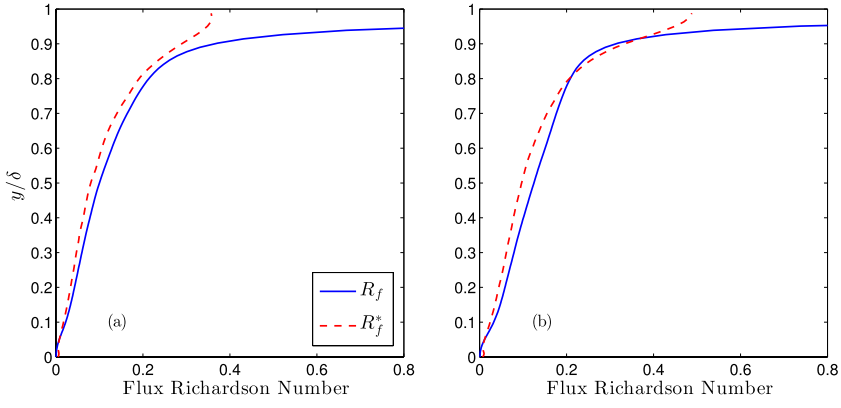

FIG. 3. Comparison of R_f and R_f^* versus depth in a turbulent channel flow with (a) $Ri_\tau = 60$ and (b) $Ri_\tau = 120$ and at $Re_\tau = 550$, computed from the DNS data of García-Villalba and del Álamo.[7] Here, δ is half of the channel depth.

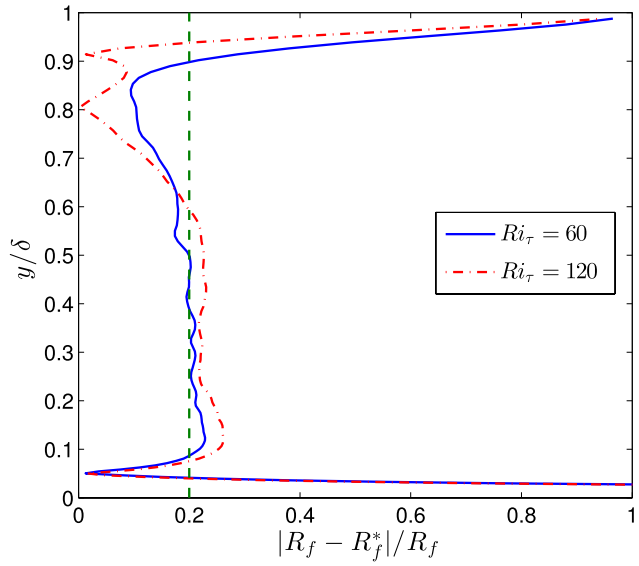

FIG. 4. Normalized difference between the flux Richardson number (R_f) and the irreversible flux Richardson number (R_f^*) versus depth in a turbulent channel flow at $Re_\tau = 550$ for $Ri_\tau = 60$ and $Ri_\tau = 120$, computed from the DNS data of García-Villalba and del Álamo.[7] Here, δ is half of the channel depth.

$P \neq \epsilon + \epsilon_{PE}$. Also, in the outer (wake) region, Ri_g increases without bound as a result of the relaxation of the mean shear rate (S). This stably stratified region supports the presence of linear internal wave motions leading to the generation of strong countergradient fluxes. Furthermore, it should be noted that the production and dissipation terms are very small in this far-wall region. As a result, the transport terms become relatively dominant causing R_f to deviate from R_f^* as shown in Figures 1, 3, and 4.

In Figure 5, the behavior of R_f versus Ri_g for two different initial stratifications is shown. It is interesting to observe from Figure 5 that the flux Richardson number (R_f) for different stratifications agrees very well when $Ri_g < 0.25$. This is in contrast to the behavior of R_f and R_f^* for high

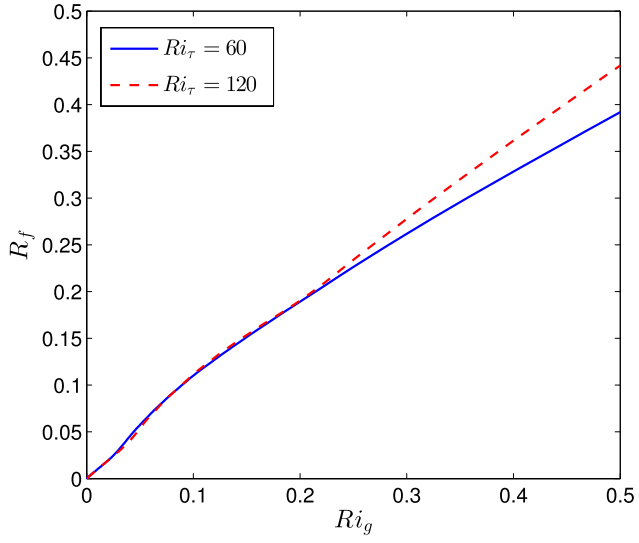

FIG. 5. R_f versus Ri_g for a turbulent channel flow at $Re_\tau = 550$ and $Ri_\tau = 60, 120$, computed from the DNS data of García-Villalba and del Álamo.[7]

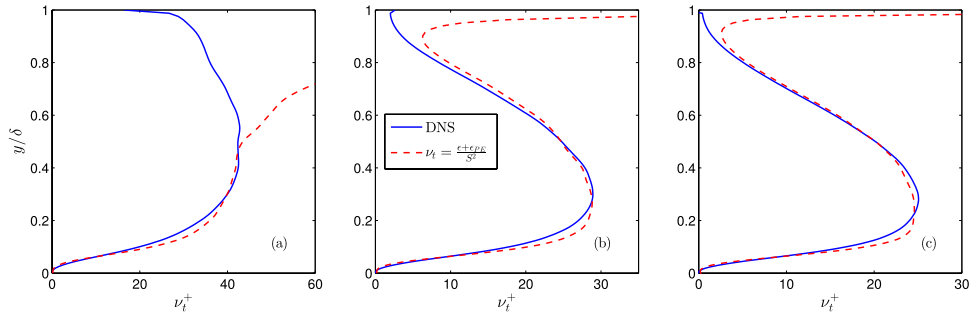

FIG. 6. Comparison of the exact turbulent viscosity and the prediction given by Eq. (23) in a turbulent channel flow at $Re_\tau = 550$ and (a) $Ri_\tau = 0$, (b) $Ri_\tau = 60$, and (c) $Ri_\tau = 120$, computed from the DNS data of García-Villalba and del Álamo.[7] Here, δ is half of the channel depth.

gradient Richardson numbers which indicate dependence on the strength of the density stratification. The key insight from this observation is that R_f and R_f^* may have a generally similar behavior as long as turbulence is sustained in stably stratified sheared flows. However, this finding needs to be investigated further using well-resolved field and experimental data as well as DNS data at higher Reynolds numbers and different stratification strengths.

B. Comparisons of the turbulent viscosity, velocity, and length scales

The comparison between the proposed turbulent viscosity from Eq. (23) and the exact turbulent viscosity given by Eq. (1) is shown in Figure 6 for initial stratifications of $Ri_\tau = 0$, 60, and 120. The predicted turbulent viscosity agrees with the exact ν_t within 95% in the equilibrium layer (i.e., here, for $0.05 \lesssim y/\delta \lesssim 0.8$ for stratified flows). This is a remarkably interesting result, especially given the fact that all the divergences of fluxes are neglected in deriving Eq. (23). This result highlights the suitability of neglecting these reversible terms in the evolution equation of k in wall-bounded flows. Moreover, it is interesting to note that while the turbulent viscosity (ν_t) of unstratified flow is predicted well for up to almost half of the flow depth ($y/\delta \lesssim 0.5$), the prediction substantially improves for most of the channel depth for the stably stratified cases. This implies that the presence of

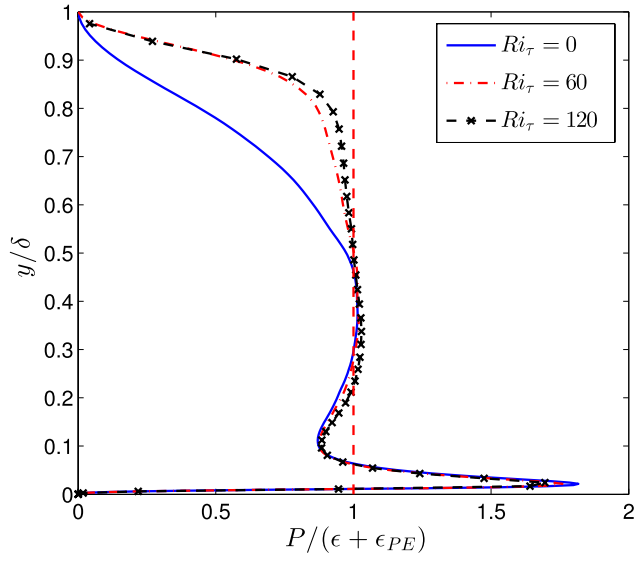

FIG. 7. Comparison of $P/(\epsilon+\epsilon_{PE})$ for different initial stratifications with $Ri_\tau = 0$, 60, and 120 in a turbulent channel flow at $Re_\tau = 550$, computed from the DNS data of García-Villalba and del Álamo.[7] Here, δ is half of the channel depth.

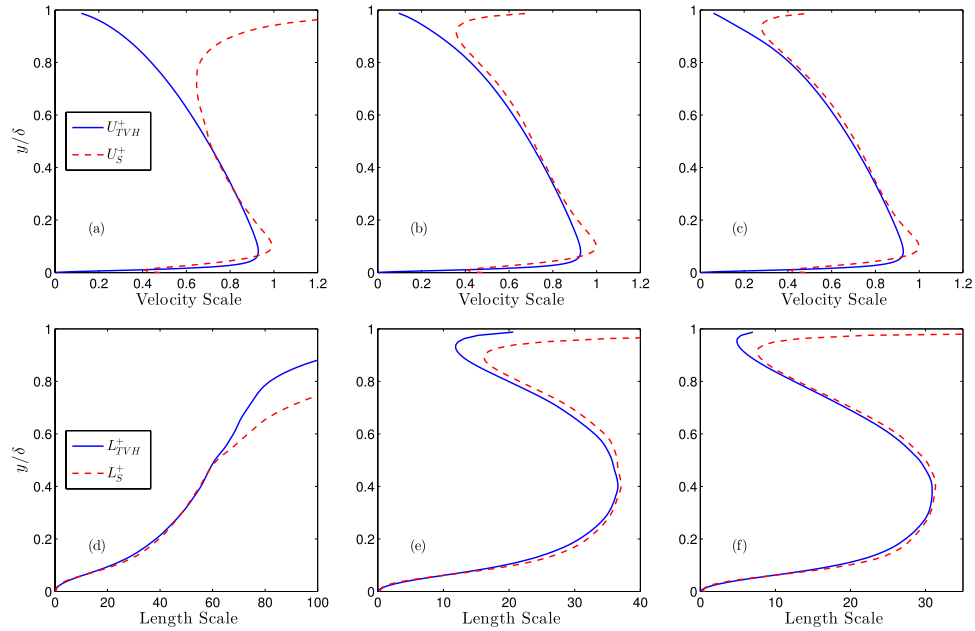

FIG. 8. Comparison of velocity scales (upper panel) and length scales (lower panel) in a turbulent channel flow at $Re_\tau = 550$: (a) and (d) $Ri_\tau = 0$; (b) and (e) $Ri_\tau = 60$; and (c) and (f) $Ri_\tau = 120$, computed from the DNS data of García-Villalba and del Álamo.[7] Here, δ is half of the channel depth.

the buoyancy fluxes in stably stratified flows appears to keep the flow in equilibrium over a greater portion of the flow depth. This can be readily seen by comparing $P/(\epsilon + \epsilon_{PE})$ for the unstratified and stratified cases as shown in Figure 7 for $Ri_\tau = 0$, 60, and 120. This confirms the assertion that $P \approx \epsilon + \epsilon_{PE}$ holds over a larger fraction of the flow depth compared to the unstratified channel flow case.

Figure 8 shows the comparison of velocity scales and length scales discussed in Sec. II C. The comparison between the exact velocity scale (U_{TVH}) and the proposed velocity scale (U_S) given by Eq. (27) is shown in Figures 8(a)–8(c) and also the corresponding comparison between L_{TVH} and L_S given by Eq. (28) is shown in Figures 8(d)–8(f). As expected, the comparison is promising and similar to the ν_t comparison, the agreement improves with increase in stratification. The agreement between L_{TVH} and L_S strengthens our earlier assertion that L_S may be considered as the pertinent length scale in stably stratified wall-bounded flows.

IV. PREDICTION OF THE TURBULENT DIFFUSIVITY

The correct prediction of the turbulent diffusivity (κ_t) is important for quantifying scalar mixing and consequently the flow dynamics. As shown in Sec. III B, the equilibrium assumption as $P \approx \epsilon + \epsilon_{PE}$ results in a good estimation for ν_t. Here, we test the suitability of employing the equilibrium assumption as $-B \approx \epsilon_{PE}$ for predicting the turbulent diffusivity in a stably stratified channel flow.

A. Equilibrium assumption

It can be seen from the evolution equations of the turbulent kinetic and turbulent potential energies (Eqs. (8) and (10)) that the buoyancy flux is present in both the turbulent kinetic energy and the turbulent potential energy evolution equations with opposite signs. This indicates that for stable density gradients, the turbulent kinetic energy is transferred via the buoyancy flux into the available potential energy. For unstable (convective) density gradients, the available potential energy can be transferred as the buoyancy flux into the turbulent kinetic energy. It must be noted that the presence

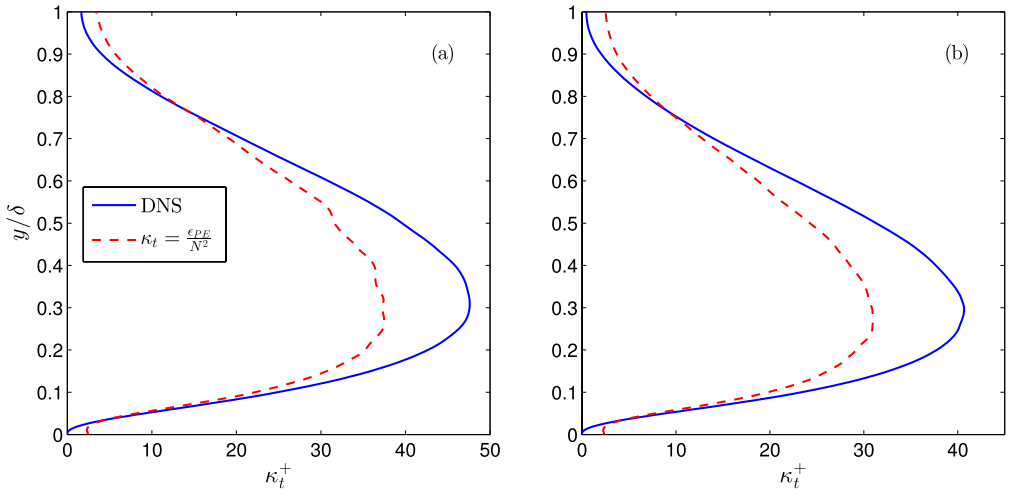

FIG. 9. Comparison of the exact turbulent diffusivity and the prediction given in Eq. (31) in a turbulent channel flow with (a) $Ri_\tau = 60$ and (b) $Ri_\tau = 120$ and at $Re_\tau = 550$, computed from the DNS data of García-Villalba and del Álamo.[7] Here, δ is half of the channel depth.

of internal wave motions can cause countergradient fluxes that transfer energy back and forth between the turbulent kinetic energy and the available potential energy. This will be discussed more in Sec. IV B.

As shown in Eq. (17), for a fully developed flow, Eq. (10) can be rearranged as

$$-B = \epsilon_{PE} - T_{PE}. \tag{29}$$

By replacing $-B = \kappa_t N^2$, the turbulent diffusivity can be derived as

$$\kappa_t = \frac{\epsilon_{PE} - T_{PE}}{N^2}. \tag{30}$$

Now, by assuming the equilibrium between the buoyancy flux (B) and the dissipation rate of the turbulent potential energy (ϵ_{PE}) as $-B \approx \epsilon_{PE}$, κ_t simplifies to

$$\kappa_t \approx \frac{\epsilon_{PE}}{N^2} = \frac{R_f^*}{1 - R_f^*} \frac{\epsilon}{N^2}. \tag{31}$$

This is the well-known Osborn and Cox[11] model. This formulation is widely employed for calculating κ_t in stably stratified flows. Given the extensive employment of this model for inference of mixing in geophysical flows, a revisit of its efficacy in wall-bounded stratified flows is warranted.

B. Testing κ_t using DNS data

Figure 9 shows the comparison between the equilibrium based formulation for κ_t given by Eq. (31) and the exact κ_t given by Eq. (2). The overall prediction of the turbulent diffusivity based on equilibrium between $-B$ and ϵ_{PE} is good close to the wall. In this region, the mean shear rate is strong and thus turbulence is vigorously sustained which results in irreversible transfer of kinetic energy to background potential energy. However, this agreement starts to break down away from the wall. This is in contrast to the predictions shown earlier for the turbulent viscosity where remarkable agreement was seen even in the far-wall region. This breakdown can be mainly attributed to the presence of linear internal waves in the far-wall region of the channel flow.

García-Villalba and del Álamo[7] analyzed the behavior of the wall-normal velocity fluctuation ($\overline{v'^2}^{1/2}$) and the density fluctuation ($\overline{\rho'^2}^{1/2}$) for the stably stratified wall-bounded flow and observed that their magnitudes are considerably high. They attributed these high root mean square values to the existence of internal wave motions in the core region of the stably stratified channel. Furthermore, by visualizing two-dimensional spectral densities at $y/\delta = 0.75$, they observed a clear

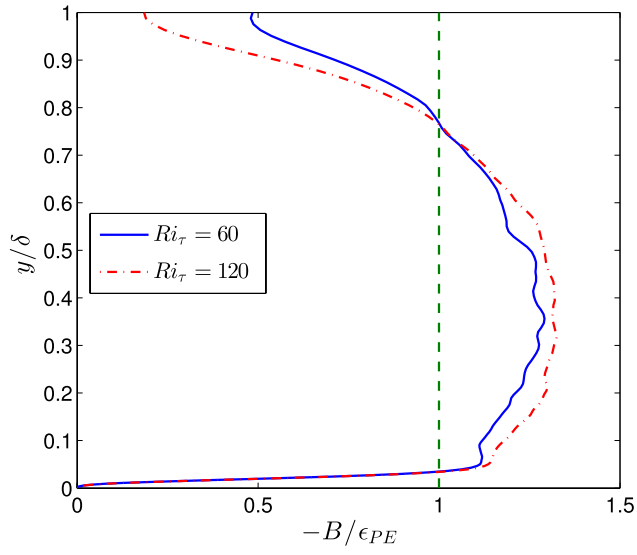

FIG. 10. Comparison of $-B/\epsilon_{PE}$ for different initial stratifications with $Ri_\tau = 60$ and 120 in a turbulent channel flow at $Re_\tau = 550$, computed from the DNS data of García-Villalba and del Álamo.[7] Here, δ is half of the channel depth.

effect of internal waves. They concluded that the buoyancy flux arises from both stratified wall turbulence and internal waves away from the wall. The result shown in Figure 9 also highlights the complexity associated with the co-existence of internal waves and turbulence in stably stratified flows. Hence, it is important to separate motions such as internal waves from fluctuating small scale turbulence since turbulent mixing is a result of small scale processes and wavelike motions have negligible contributions to irreversible mixing.[23] However, separating wave and turbulence in such flows remains an important challenge. Given the breakdown in agreement between actual turbulent diffusivity given by Eq. (2) and the Osborn-Cox[11] model (as given by Eq. (31)), it is necessary to exercise caution when using the Osborn-Cox[11] model for inferring the total diffusivity for modeling purposes (i.e., inference of buoyancy flux) or vice versa where irreversible mixing is inferred from the buoyancy flux.

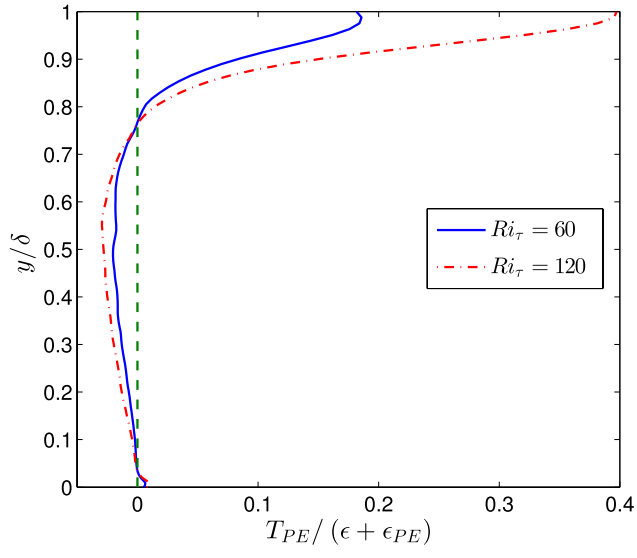

FIG. 11. Comparison of $T_{PE}/(\epsilon + \epsilon_{PE})$ for different initial stratifications with $Ri_\tau = 60$ and 120 in a turbulent channel flow at $Re_\tau = 550$, computed from the DNS data of García-Villalba and del Álamo.[7] Here, δ is half of the channel depth.

In order to better investigate the validity of assuming equilibrium between ϵ_{PE} and $-B$, it will be instructive to revisit $-B/\epsilon_{PE}$ which shows the ratio of the production to dissipation rates of the turbulent potential energy. This ratio can be considered to be equivalent to $P/(\epsilon + \epsilon_{PE})$ in the evolution equation of k. $-B/\epsilon_{PE}$ behavior is shown in Figure 10 which clearly shows that unlike $P/(\epsilon + \epsilon_{PE}) \approx 1$ which holds over a big fraction of the flow depth (Figure 7), an equilibrium region, where $-B \approx \epsilon_{PE}$, can be barely observed in stably stratified wall-bounded flows.

The lack of equilibrium shown in Figure 10 (i.e., $-B \neq \epsilon_{PE}$) means that T_{PE} is not negligible compared to ϵ_{PE} in Eq. (17). Such a result might question the suitability of assuming equilibrium for deriving Eqs. (22) and (23). This lack of equilibrium is also the reason for the differences between R_f and R_f^* as discussed in Sec. III A, particularly in the free-stream region. It should be noted that although T_{PE} is not negligible compared to ϵ_{PE} as shown in Figure 10, it is much smaller than the total dissipation rate (i.e., $\epsilon_T = \epsilon + \epsilon_{PE}$) as shown in Figure 11, where $T_{PE}/(\epsilon + \epsilon_{PE})$ is very small (less than 5%), except near the free-stream region. This is the reason why ν_t can be predicted very well using Eq. (23).

V. CONCLUDING REMARKS

In this study, we have revisited the suitability of the equilibrium (irreversibility) assumption (i.e., $P \approx \epsilon + \epsilon_{PE}$ and $-B \approx \epsilon_{PE}$) for estimating the irreversible flux Richardson number (R_f^*), turbulent viscosity (ν_t), and turbulent diffusivity (κ_t) in a stably stratified channel flow. We have first shown by using DNS data that the flux Richardson number defined as $R_f = -B/P$ and the irreversible flux Richardson number ($R_f^* = \epsilon_{PE}/(\epsilon + \epsilon_{PE})$) which is derived from R_f by assuming equilibrium show reasonable comparison for $Ri_g \lesssim 0.25$.

We then invoked the equilibrium assumption between P, ϵ, and ϵ_{PE} to propose that $\nu_t \approx 1/(1 - R_f^*)(\epsilon/S^2)$. We then used dimensional arguments to show that the appropriate velocity scale is $U_S = (1 - R_f^*)^{-1/2}(\epsilon/S)^{1/2}$ and the appropriate length scale is $L_S = (1 - R_f^*)^{-1/2}(\epsilon/S^3)^{1/2}$, respectively. The comparisons of the proposed turbulent viscosity and the relevant scales with the exact turbulent viscosity and scales computed from the DNS data of stably stratified turbulent channel flow are remarkably good. Interestingly, it is observed that the comparisons become better when the stratification strength increases which implies that in stratified wall-bounded flows, the equilibrium assumption as $P \approx \epsilon + \epsilon_{PE}$ holds for a bigger fraction of the flow depth compared to the unstratified counterpart.

Finally, we have tested the suitability of assuming equilibrium for predicting κ_t. This is done by invoking the equilibrium assumption between the buoyancy flux (B) and the dissipation rate of the turbulent potential energy (ϵ_{PE}) (i.e., $-B \approx \epsilon_{PE}$) to propose that $\kappa_t \approx \epsilon_{PE}/N^2$. The comparison of the proposed turbulent diffusivity with the exact turbulent diffusivity computed from the DNS data is good close to the wall. However, unlike the prediction of the turbulent viscosity, the results show that the agreement deteriorates far from the wall. This can be attributed to the presence of linear internal waves in the far-wall region that cause advective fluxes that do not contribute to irreversible turbulent mixing. Future DNS studies of stably stratified channel flows at higher Reynolds numbers are required in order to test the sensitivity of the predictions presented in this study.

ACKNOWLEDGMENTS

The authors thank the two anonymous referees for their constructive comments and recommendations. We would like to thank Dr. M. García-Villalba, Dr. J. C. del Álamo, and Dr. A. Scotti for providing their detailed post-processed DNS results for the stratified channel flow. We also gratefully acknowledge the support from the National Science Foundation under CAREER Grant No. OCE-1151838 (Program Director: Dr. E. Itsweire). S.K.V. also gratefully acknowledges the support of the Office of Naval Research under Grant No. N00014-12-1-0938 (Scientific officers: Dr. Terri Paluszkiewicz and Dr. Scott Harper).

[1] S. P. S. Arya, "Buoyancy effects in a horizontal flat-plate boundary layer," J. Fluid Mech. **68**, 321–343 (1975).
[2] S. Komori, H. Ueda, F. Ogino, and T. Mizushina, "Turbulence structure in stably stratified open-channel flow," J. Fluid Mech. **130**, 13–26 (1983).

[3] R. P. Garg, J. H. Ferziger, S. G. Monismith, and J. R. Koseff, "Stably stratified turbulent channel flows. I. Stratification regimes and turbulence suppression mechanism," Phys. Fluids **12**, 2569–2594 (2000).
[4] V. Armenio and S. Sarkar, "An investigation of stably stratified turbulent channel flow using large-eddy simulation," J. Fluid Mech. **459**, 1–42 (2002).
[5] F. T. M. Nieuwstadt, "Direct numerical simulation of stable channel flow at large stability," Boundary-Layer Meteorol. **116**, 277–299 (2005).
[6] J. R. Taylor, S. Sarkar, and V. Armenio, "Large eddy simulation of stably stratified open channel flow," Phys. Fluids **17**, 116602 (2005).
[7] M. García-Villalba and J. C. del Álamo, "Turbulence modification by stable stratification in channel flow," Phys. Fluids **23**, 045104 (2011).
[8] W. Rodi, "Examples of calculation methods for flow and mixing in stratified fluids," J. Geophys. Res.: Oceans **92**, 5305–5328 doi:10.1029/JC092iC05p05305 (1987).
[9] F. Karimpour and S. K. Venayagamoorthy, "A revisit of the equilibrium assumption for predicting near-wall turbulence," J. Fluid Mech. **760**, 304–312 (2014).
[10] W. R. Peltier and C. P. Caulfield, "Mixing efficiency in stratified shear flows," Annu. Rev. Fluid Mech. **35**, 135–167 (2003).
[11] T. R. Osborn and C. S. Cox, "Oceanic fine structure," Geophys. Fluid Dyn. **3**, 321–345 (1972).
[12] K. B. Winters and E. A. D'Asaro, "Diascalar flux and the rate of fluid mixing," J. Fluid Mech. **317**, 179–193 (1996).
[13] E. Lindborg and E. Fedina, "Vertical turbulent diffusion in stably stratified flows," Geophys. Res. Lett. **36**, L01605 doi: 10.1029/2008GL036437 (2009).
[14] F. Karimpour and S. K. Venayagamoorthy, "A simple turbulence model for stably stratified wall-bounded flows," J. Geophys. Res.: Oceans **119**, 870–880 doi:10.1002/2013JC009332 (2014).
[15] S. K. Venayagamoorthy and D. D. Stretch, "On the turbulent Prandtl number in homogeneous stably stratified turbulence," J. Fluid Mech. **644**, 359–369 (2010).
[16] S. B. Pope, *Turbulent Flows* (Cambridge University Press, 2000).
[17] A. A. Townsend, "Equilibrium layers and wall turbulence," J. Fluid Mech. **11**, 97–120 (1961).
[18] S. Corrsin, "Local isotropy in turbulent shear flow," NACA RM 58B11, 1958, pp. 1–15.
[19] F. Karimpour and S. K. Venayagamoorthy, "Some insights for the prediction of near-wall turbulence," J. Fluid Mech. **723**, 126–139 (2013).
[20] J. W. Miles, "On the stability of heterogeneous shear flows," J. Fluid Mech. **10**, 496–508 (1961).
[21] L. N. Howard, "Note on a paper of John W. Miles," J. Fluid Mech. **10**, 509–512 (1961).
[22] B. Galperin, S. Sukoriansky, and P. S. Anderson, "On the critical Richardson number in stably stratified turbulence," Atmos. Sci. Lett. **8**, 65–69 (2007).
[23] T. R. Osborn, "Estimates of the local rate of vertical diffusion from dissipation measurements," J. Phys. Oceanogr. **10**, 83–89 (1980).